Supporting Information for: Modulation of Single Photon Emission from Suspended 1L WSe_2 under Electrostatically Induced Strain

Frances Camille M. Wu,[†,‡] Shang-Hsuan Wu,[†] Bin Fang,[‡] Xintong Li,[†,‡] Jadon Zheng,[†,‡] Jean Anne C. Incorvia,[†,‡] and Edward T. Yu[*,†,‡]

†Chandra Family Department of Electrical and Computer Engineering, The University of Texas at Austin, Austin, TX 78758, United States

‡Center for Dynamics and Control of Materials, The University of Texas at Austin, Austin, TX 78758, United States

*Corresponding Author: Edward T. Yu – Email: ety@ece.utexas.edu

Supporting Note 1: *Fabrication of cavity-patterned substrates*

The device was fabricated, as shown in **Figure S1**. First, substrates patterned with an array of cavities were prepared using nanosphere lithography. Briefly, a hexagonal close-packed monolayer of 3-μm diameter PS microspheres (Polysciences Inc.) was formed using a sequential injection of the PS microspheres onto an air-water interface using a pipette tip.[1-2] Afterwards, the

reservoir was drained and air dried at room temperature for 24 h to form a self-assembled monolayer of PS

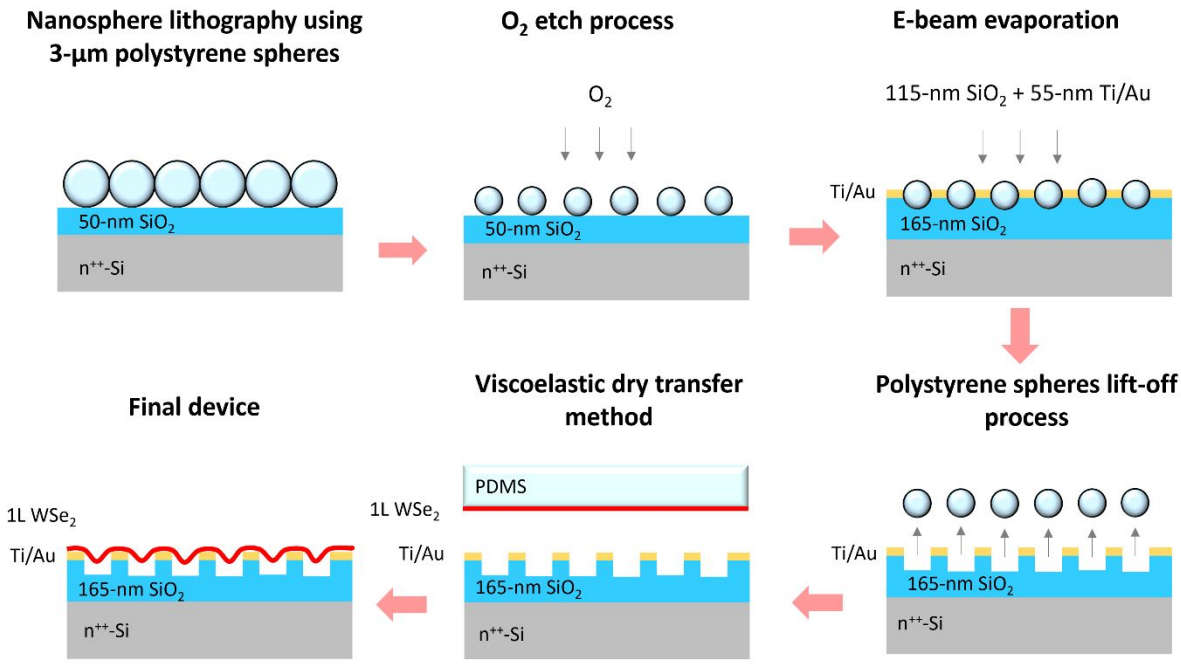

Figure S1. Schematic diagram of the device fabrication process of a substrate patterned with a hexagonal array of cavities using nanosphere lithography. The 1L WSe_2 is transferred to the final device using the viscoelastic dry transfer method.

microspheres on SiO_2(50 nm)/Si substrates. Second, the deposited PS microspheres on SiO_2(50 nm)/Si substrates were partially etched using reactive ion etching with an O_2 plasma process to reduce the PS microspheres diameter from 3-µm to 1.65–2 µm, creating gaps between the microspheres and thereby enabling the fabrication of an array of separated cavities. Third, 100-nm SiO_2 and 55-nm thick Ti/Au were deposited on the nanosphere-patterned SiO_2/Si substrates using electron beam evaporation. The 50-nm Au film serves as the top contact electrode, and the Si substrate acts as the bottom electrode. The total thickness of the evaporated materials defines

the total cavity depth. Fourth, the PS microsphere masks were lifted off using a sonication process with toluene, and the sample was then dried using compressed nitrogen gas.[1] The cavity-patterned substrates were characterized using an atomic force microscope (AFM Bruker Icon) to determine the final cavity dimensions. Finally, a mechanically exfoliated WSe_2 monolayer was transferred to the cavity-patterned substrates using a viscoelastic dry transfer method. Afterward, the final device was silver pasted to a sample mount with multiple pins, and two wire bonds were connected – one for the Au film, which is connected to the WSe_2 (top electrode), and another for the Si substrate (bottom electrode). The final vertical resistance of the overall device was measured using a multimeter probe, showing a typical resistance value of ≥ 50 MΩ.

Supporting Note 2: *Modeling of electrostatically induced deflection of suspended 1L WSe_2*

To determine the cavity dimensions needed to create a sufficient amount of strain at accessible bias voltages, model calculations were performed assuming a semi-spherical monolayer deflection geometry. This approximation is valid for deflections, z_0, that are small compared to the cavity radius r. We first calculated the radial component of the strain tensor, ε_{rr}, which corresponds to the change in radial length due to radial displacement and is given by

$$\varepsilon_{rr} = \frac{2}{3}\frac{{z_0}^2}{r^2} \ , \qquad (\boldsymbol{S1})$$

where z_0 is the monolayer deflection, and r is the cavity radius. By calculating the upward force due to strain (F_{str}) and the downward force due to electrostatic interactions (F_{el}), we estimate the applied voltage, V_g, required to produce deflection, z_0, to be

$$V_g = \left[(5 \times 10^{13}) \frac{z_0^3 \left(d - \frac{1}{2} z_0\right)^2}{r^4} \right]^{1/2}, \qquad (\boldsymbol{S2})$$

where r is the cavity radius in nm, and d is the cavity depth, also in nm.

Figures S2a and S2b show the monolayer deflection and strain as functions of applied voltage calculated using **Equations** (**S1**) and (**S2**) at different cavity diameters. Based on the calculated results, larger diameters would require larger deflections to induce a given level of tensile strain in 1L WSe_2. For example, at r = 1250 nm, 0.4% strain is achieved at 100 nm monolayer deflection, while at r = 825 nm, a 100-nm monolayer deflection would result in 1% strain in the monolayer (see **Figure S2c**). Although large diameter cavities require less applied bias to achieve a given strain level (see **Figures S2a** and **S2b**), larger deflections are needed to achieve the same strain level (see **Figure S2c**), which is less practical for device design. On the other hand, while smaller cavity diameters (r ≤ 500 nm) would require smaller deflections at a relatively higher applied bias (see **Figures S2a** and **S2b**) for a given strain level, significant optical contributions from flat, unstrained areas (bright neutral excitons) would make a substantial contribution to the PL emission given our excitation laser spot size (FWHM = 1.22 μm). Thus, a cavity radius r = 825 nm is chosen, wherein PL emission from highly strained areas (dark excitons) at the center of the cavity would dominate. At r = 825 nm, a 45-nm monolayer deflection is predicted to be achievable at 15 V gate bias and to correspond to a 0.2% increase in tensile strain of the suspended 1L WSe_2 (see **Figures S2a** and **S2b**). This strain value is sufficient for investigating localized emitters associated with quantum emitters based on strained 1L WSe_2.[3-4]

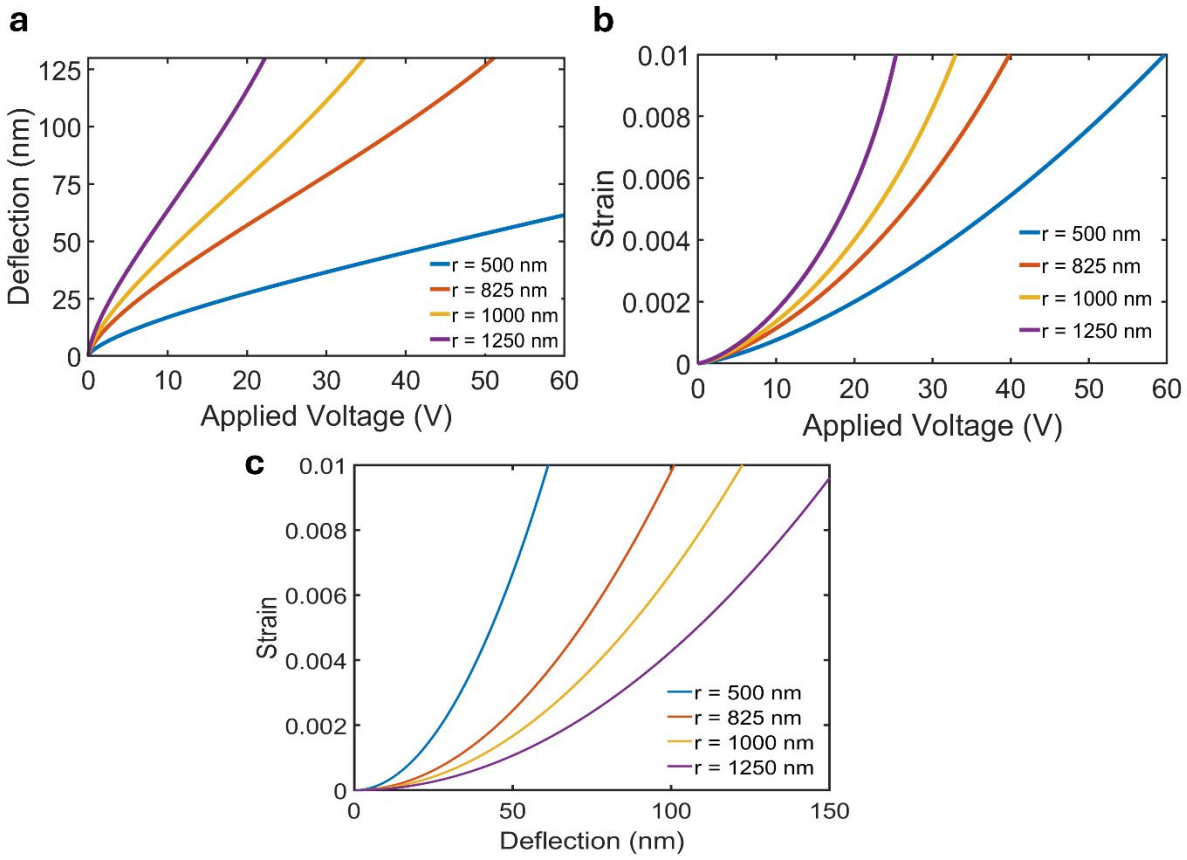

Figure S2. Modeling of electrostatically induced deflection of suspended 1L WSe_2. a, b) Calculated monolayer deflection (a) and strain (b) as functions of applied voltage, assuming a semi-spherical monolayer deflection geometry. c) Calculated strain as a function of monolayer deflection.

Supporting Note 2a: *Derivation of strain using electrostatic deflection*

Assuming a circumferential geometry of the WSe_2 monolayer suspended over a single-cavity patterned substrate (see Figure S5 (left)), three points on a circle are known, namely (-r, 0), (0, -z), and (r, 0) (see Figure S5 (right)). The calculated radius of curvature, *R*, is given by,

$$R = \frac{r^2 + z^2}{2z}$$

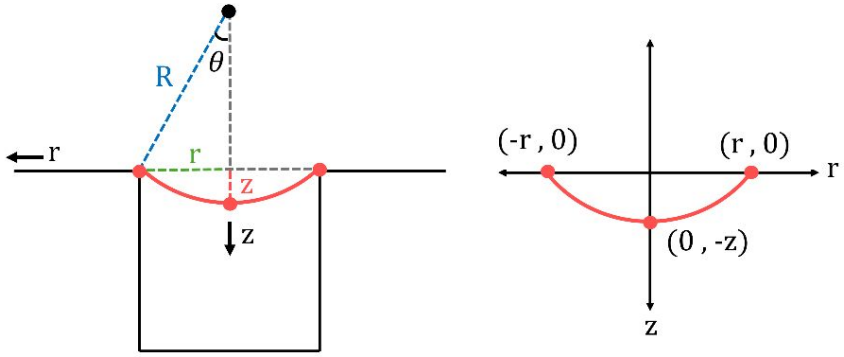

Figure S3. A schematic diagram showing a circular WSe_2 monolayer geometry suspended over a single cavity patterned substrate (left) and the corresponding positions of three points on a circle (right).

where r is the cavity radius and z is the monolayer deflection. To calculate the radial component of the strain tensor, ε_{rr}, we first calculated the arc length deduced from the schematic diagram shown in Figure S5 (left),

$$arc\ length\ = \left[\frac{r^2 + z^2}{2z}\right] sin^{-1}\left[\frac{2zr}{r^2 + z^2}\right]$$

Given an initially flat, unstrained WSe_2 monolayer film, the strain is approximated as the change in arc length divided by the original arc length. Therefore, the radial component of the strain tensor, ε_{rr}, can be estimated using,

$$\varepsilon_{rr} = \frac{\left[\frac{r^2 + z^2}{2z}\right] sin^{-1}\left[\frac{2zr}{r^2 + z^2}\right] - r}{r}$$

which can be further simplified for z << r as,

$$\varepsilon_{rr} = \frac{2}{3}\frac{z^2}{r^2}$$

Supporting Note 2b: *Estimation of applied voltage for monolayer deflection*

To estimate the applied voltage required to produce a given level of monolayer deflection, two forces acting on the suspended WSe_2 monolayer were considered: the upward force due to strain energy (F_{str}) and the downward force due to electrostatic interactions (F_{el}). The upward force due to strain, F_{str}, can be estimated by first calculating the total strain energy, U_{str},

$$U_{str} = \frac{1}{2}C_{ij}\varepsilon_i\varepsilon_j$$

$$U_{str} = \frac{1}{2}C_{ij}\varepsilon^2$$

$$U_{str} = \frac{2\pi}{9}C\frac{z^4}{r^2}$$

where C_{ij} is the elastic constant of monolayer WSe_2, assuming the condition to satisfy for 2D materials to be isotropic $C_{11} \approx C_{22} \approx C$ and ε is the radial component of the strain tensor. Thus, the upward force due to strain energy is estimated using,

$$F_{str} = \frac{dU_s}{dz}$$

$$F_{str} = \frac{8\pi}{9}C\frac{z^3}{r^2}$$

On the other hand, the downward force due to electrostatic interactions, F_{el}, can be estimated by first calculating the total electrostatic energy, U_{el},

$$U_{el} = \frac{1}{2}CV^2 \, , where \; C = \frac{\varepsilon_0 A}{d - \frac{1}{2}z}$$

$$U_{el} = \frac{1}{2}\left[\frac{\varepsilon_0 \pi r^2}{d - \frac{1}{2}z}\right]V^2$$

where U_{el} is the electrostatic energy stored in a capacitor measured in Joules (J), C is the capacitance measured in Farad (F), and V is the voltage in volts (V). Here, the capacitance is estimated assuming a simple planar geometry where two electrically conductive plates are separated by a dielectric insulating material (valid for z << r), where ε_0 is the permittivity, A is the area assuming a circular geometry, d is the distance between two conductive plates, also known as cavity depth, and z is the monolayer deflection.

Therefore, the downward force due to electrostatic interactions is given by,

$$F_{el} = \frac{dU_{el}}{dz}$$

$$F_{el} = \frac{1}{4}\left[\frac{\varepsilon_0 \pi r^2}{\left(d - \frac{1}{2}z\right)^2}\right]V^2$$

In equilibrium, taking into account the two forces: the upward force due to strain energy and the downward force due to electrostatic interactions,

$$F_{el} = F_{str}$$

Thus, the applied bias in volts (V), V_g, required to produce deflection, z, in nm to be

$$V_g = \left[(5 \times 10^{13}) \frac{z^3 \left(d - \frac{1}{2} z \right)^2}{r^4} \right]^{1/2}$$

where r is the cavity radius in nm and d is the cavity depth, also in nm.

Supporting Note 3: *Characterization of 1L WSe_2 suspended over cavity-patterned substrate*

An AFM topographic image of a patterned substrate shows an array pitch of 3 μm and a cavity diameter of 1.65 μm (see **Figure S4a**). The pitch of 3 μm is determined by the original polystyrene (PS) microsphere diameter before the O_2 etch process. Based on the model calculations shown in **Figures S2a** and **S2b**, a 1.65 μm cavity diameter is ideal for electrostatic strain control of suspended 1L WSe_2, and this diameter is achieved after 15 minutes of O_2 plasma etching (see **Figure S1**). The AFM topographic image and the corresponding depth profile shown in **Figures S4b** and **S4c** reveal a cavity depth of 170 nm, which is in good agreement with the thickness of the evaporated materials (see **Figure S1**). An initial sagging of the suspended 1L WSe_2 is also observed, which we attribute to the strain that the monolayer experienced during the transfer process from PDMS to the patterned substrate. This initial monolayer sagging can range from approximately 30 to 40 nm, depending on the amount of pressure the monolayer experiences during the transfer process. Considering the ~40 nm initial sag of the monolayer, a 170 nm cavity depth is ideal for electrostatically deflecting the suspended 1L WSe_2 to create a tensile strain of

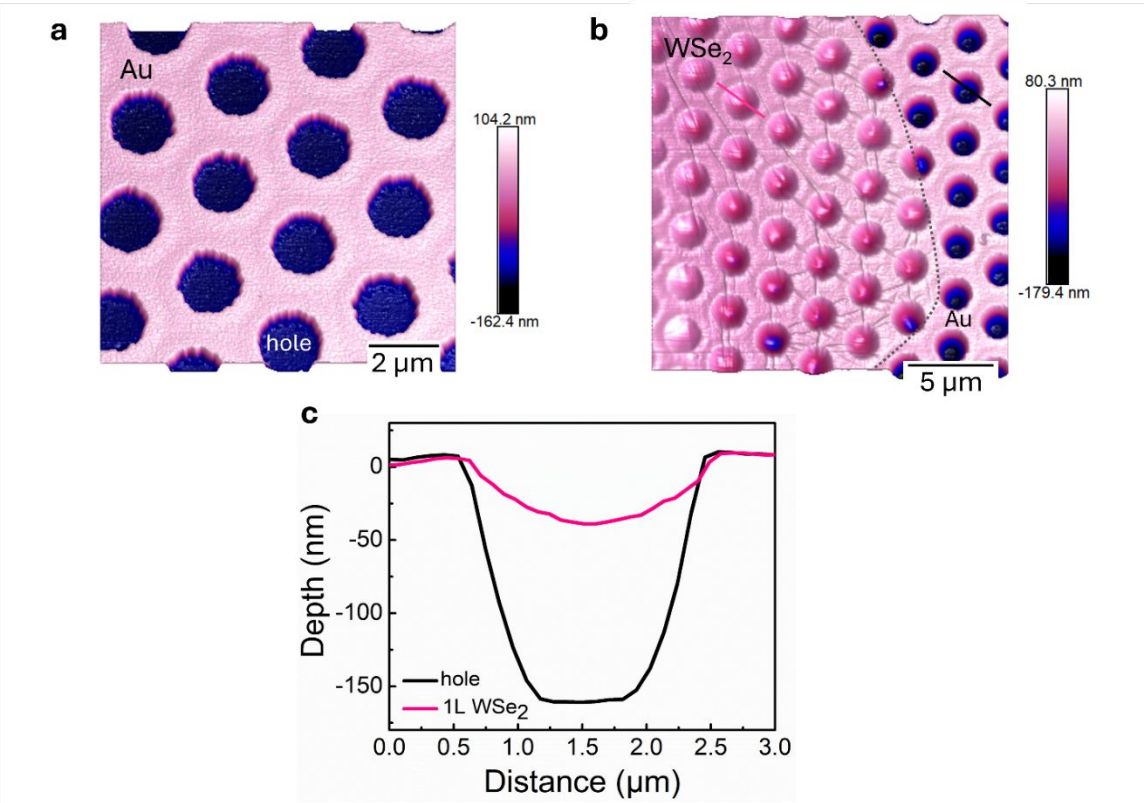

Figure S4. Characterization of 1L WSe_2 suspended over a substrate patterned with an array of cavities. a) AFM topographic image of the fabricated patterned substrate with a cavity diameter of 1.65 µm and array pitch of 3 µm. b) AFM topographic image of the final device after the 1L WSe_2 transfer onto the patterned substrate. c) Topographic profile along lines indicated in (b) showing an initial 1L WSe_2 sagging after the transfer process and clear suspension of the 1L WSe_2 above the bottom of the cavity.

0.2−0.4%. This cavity depth ensures a sufficient distance between the 1L WSe_2 and the bottom of the cavity for deflection while still enabling electrostatic interactions.

For the electrostatic deflection measurements at room temperature, the actual monolayer deflection was measured using an atomic force microscope (AFM Bruker Icon) system operating

in tapping mode. AFM measurements were carried out at room temperature with air as the ambient. The sample was loaded to a sample stage, and connections were made at the Si back gate (signal) and Au top electrode (ground) for sample bias. Sample bias was performed using bias voltages ranging from V_g = 0 V to V_g = 15 V (see Figure 2 in the main text).

Supporting Note 4: *Optical measurements at low temperatures (T = 100 K and T = 4 K)*

The sample was loaded into a Montana Cryostat with a platform temperature of 3.5 K. A 100x 0.7 NA microscope objective was used for the excitation and collection of photoluminescence from WSe_2 monolayers. A 532 nm excitation laser, operating in CW mode, was used for excitation for PL measurements, and a 408 nm pulsed laser with a repetition rate of 40 MHz was used for time-resolved PL measurements. The collected PL was directed to a long pass filter to filter out the excitation light and was dispersed by a diffraction grating with 1200 lines/mm and recorded by a spectrometer (Andor Spectrometer) for PL measurements. For time-resolved PL measurements, two angle-tunable filters were used to set a spectral window and isolate a specific emitter, which was collected with a single-mode fiber and directed to a superconducting nanowire single-photon detector system (IDQ 281). Sample bias was performed using a DC power supply (Keithley 2400 source meter) with bias voltages ranging from V_g = 0 V to V_g = ±30 V. For second-order correlation measurements, a Hanbury-Brown and Twiss optical setup was adapted. The single emitter was isolated using tunable long-pass and short-pass filters. The isolated emitter was then directed to a beam-splitter optical fiber and detected by two superconducting nanowire single-photon detectors (IDQ 281).

Supporting Note 5: *Reproducibility of dark exciton energy shift at T = 100 K and classical light background suppression at T = 4 K*

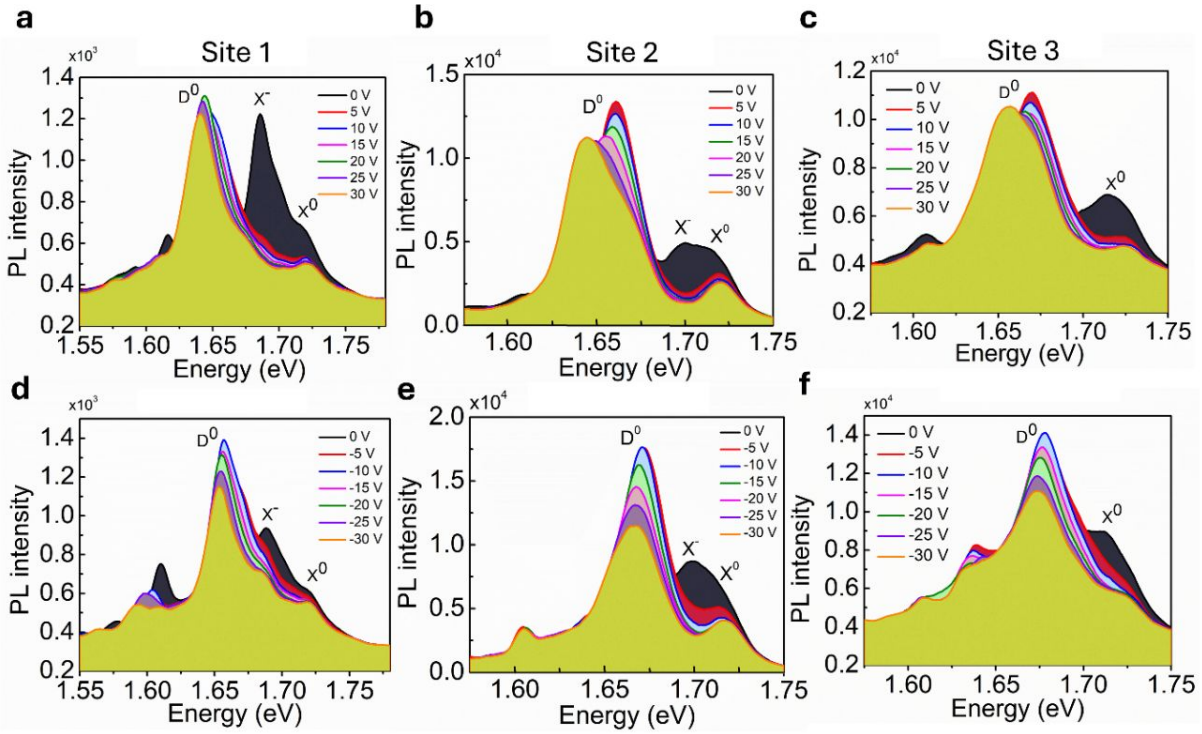

Figure S5. Photoluminescence intensity spectra at three cavity sites measured at T = 100 K.

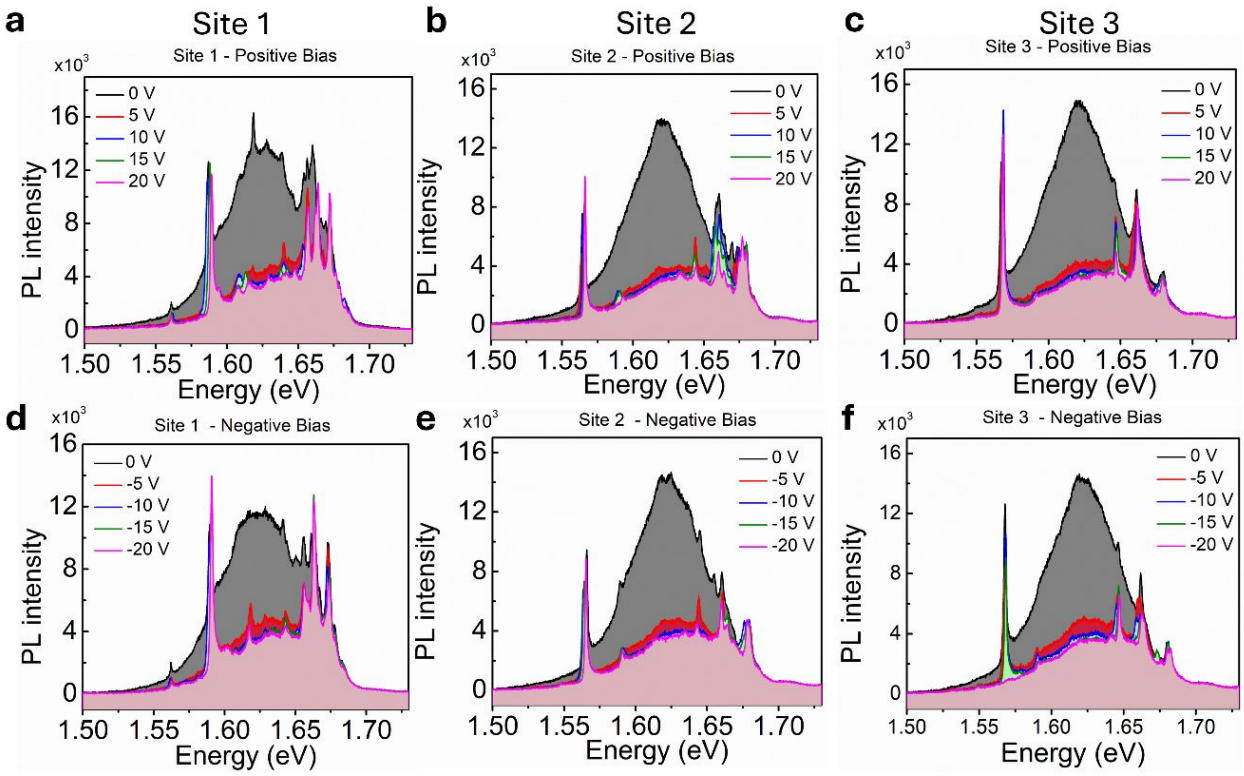

Figure S6. Classical light background reduction at three cavity sites measured at T = 4 K.

Supporting Note 6: *Temperature-dependent photoluminescence and second-order correlation*

Figure S7 shows the temperature-dependent photoluminescence and second-order correlation of the sharp localized emitters. As shown in the temperature-dependent photoluminescence spectra, sharp localized emission peaks with energies of 1.55–1.65 eV emerge at T = 10 K, and the emission peaks become narrower at T ≤ 6 K (see Figure S7a). Based on the second-order correlation measured at T = 4 K and T = 6 K, a $g^{(2)}(0) \leq 0.5$ is only achieved at T = 4 K, and the single photon purity decreases at T = 6 K (see Figure S7b and c). Therefore, all the second-order correlation measurements performed in this study were measured at T = 4 K.

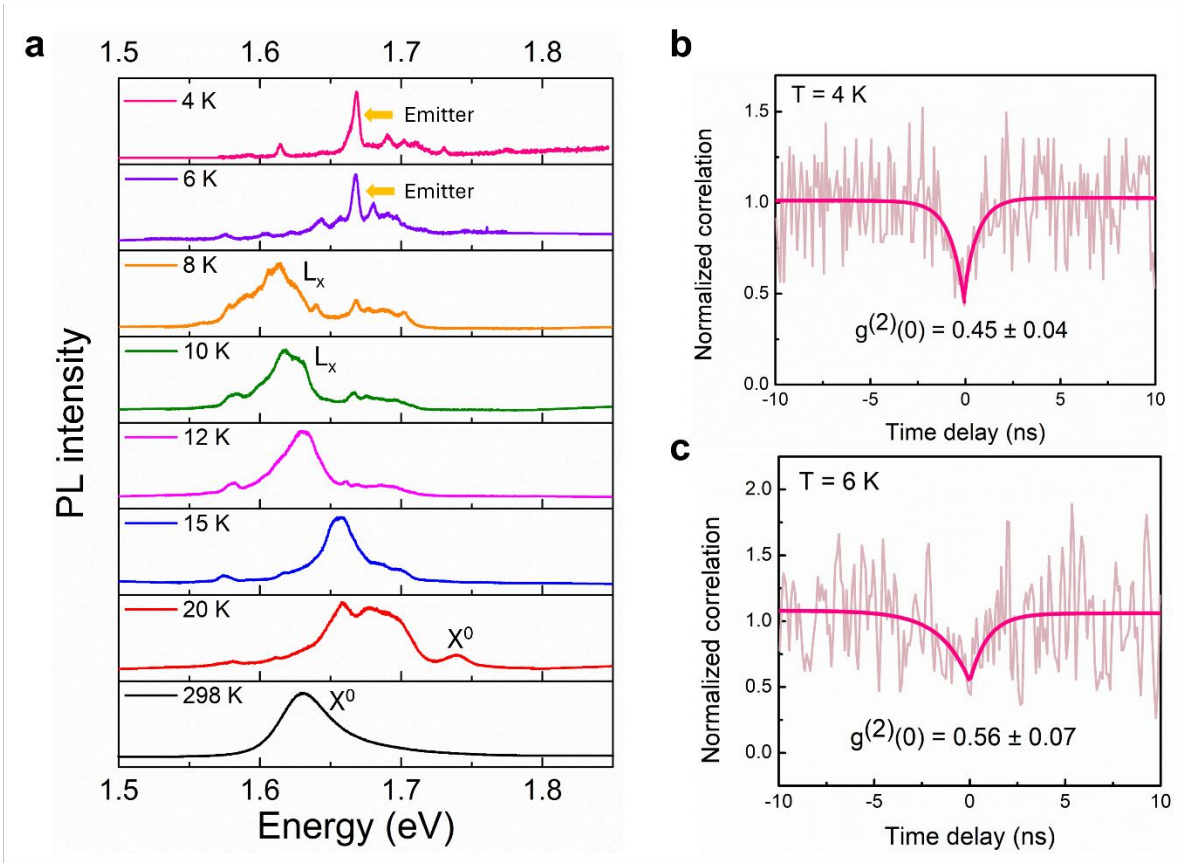

Figure S7. Temperature-dependent photoluminescence and second-order correlation of sharp localized emitters. a) Photoluminescence intensity spectra measured at different temperatures, showing the presence of sharp localized emitters at T = 10 K. X^0: bright neutral exciton, L_x: localized exciton. b, c) Second-order correlation of the chosen sharp localized emitter in (a) measured at T = 4 K (b) and T = 6 K (c), showing the decrease in single photon purity at a temperature higher than T = 4 K.

References

1. Wu, S.-H.; Cossio, G.; Braun, B.; Wu, F. C. M.; Yu, E. T., Smart Window Structures Based on Highly Conductive, Transparent Metal Nanomeshes and Thermochromic Perovskite Films. *Advanced Optical Materials* **2023,** *11* (6), 2202409.

2. Cossio, G.; Yu, E. T., Zeta Potential Dependent Self-Assembly for Very Large Area Nanosphere Lithography. *Nano Letters* **2020,** *20* (7), 5090-5096.

3. So, J.-P.; Jeong, K.-Y.; Lee, J. M.; Kim, K.-H.; Lee, S.-J.; Huh, W.; Kim, H.-R.; Choi, J.-H.; Kim, J. M.; Kim, Y. S.; Lee, C.-H.; Nam, S.; Park, H.-G., Polarization Control of Deterministic Single-Photon Emitters in Monolayer WSe2. *Nano Letters* **2021,** *21* (3), 1546-1554.

4. Kim, H.; Moon, J. S.; Noh, G.; Lee, J.; Kim, J.-H., Position and Frequency Control of Strain-Induced Quantum Emitters in WSe2 Monolayers. *Nano Letters* **2019,** *19* (10), 7534-7539.